Irregular Acoustic Streaming Formation in Symmetrically Heated Enclosures

Murat K. Aktas

***Abstract* – A numerical investigation was carried out in order to predict the effects of symmetric heating on irregular acoustic streaming in air-filled shallow enclosures. The fluid motion is driven by periodic vibration of the enclosure left wall. The vertical walls of the enclosure are adiabatic while the horizontal walls are heated symmetrically. A control-volume method based, explicit time-marching Flux-Corrected Transport Algorithm is used to simulate the transport phenomena in the enclosure. A symmetric temperature gradient strongly alters the irregular acoustic streaming structures and velocities.**

***Index Terms* – Acoustic streaming, pressure wave, enclosure**

I. INTRODUCTION

A pressure wave field in a fluid can generate a secondary, steady circulatory flow termed as acoustic streaming. Acoustic streaming can enhance heat transfer and mixing. The acoustic streaming phenomenon has been extensively studied by using theoretical and experimental methods. However, the investigations on irregular acoustic streaming structures and effect of various parameters on irregular streaming are relatively scarce. Merkli and Thomann [1] observed irregular circulations in a Stokes layer resulting from the transition to turbulence and obtained a critical Reynolds number (with present nomenclature, $2u_{max}/(\nu\omega)^{1/2} \cong 400$). Kawahashi and Arakawa [2] numerically studied acoustic streaming in a closed duct. They predicted shock wave propagation due to finite amplitude oscillations and distortion of the streaming structures. Yano [3] performed computational study of acoustic streaming formed by resonant oscillations with shock waves in a gas filled tube. For high streaming Reynolds numbers, irregular streaming patterns having vortices of various scales were predicted. Menguy and Gilbert [4] presented a comparison of slow and nonlinear acoustic streaming. The study focused on the distortion of the streaming field due to fluid inertia. A perturbation calculation using asymptotic expansions was performed and the unsymmetrical pattern of fast streaming was demonstrated. Alexeev and Gutfinger [5] investigated the periodic gas oscillations in closed tubes experimentally and numerically. They reported shock waves propagating along the tube.

Manuscript received March 16, 2012; revised April 11, 2012.
Murat K. Aktas is with TOBB University of Economics and Technology, Ankara, 06560 TURKEY (phone: +90-312-2924086, e-mail: maktas@etu.edu.tr).

Aktas and Farouk [6] carried out a computational study to determine the influence of the wave form on streaming patterns in a two dimensional enclosure. For sharp pressure gradients, irregular streaming patterns were predicted.

The influence of temperature gradients on acoustic streaming flows has been studied by several researchers. Thompson and Atchley [7] conducted acoustic and streaming velocity measurements in an air-filled cylindrical resonator by employing laser Doppler anemometry technique. Using this experimental method, Thompson et al. [8] investigated the effects of a thermoacoustically induced axial temperature gradient and fluid inertia on the acoustic streaming generated in the resonator. A strong dependence between the temperature gradient and the streaming structures was reported. The streaming velocities decrease with increasing temperature gradient and the distortion of the streaming patterns is observed. Nabavi et al. [9, 10] used particle image velocimetry technique to measure acoustic and streaming velocities in a rectangular channel carrying a standing wave. Using particle image velocimetry method, Lee and Loh [11] visualized the acoustic streaming generated by longitudinal vibrations and measured the cooling of a heat source. The effects of a transverse temperature gradient on acoustic streaming velocity fields in a rectangular enclosure were investigated by Nabavi et al. [12, 13] experimentally. It is found that the streaming velocities increase as the temperature difference between the top and the bottom walls increases. The temperature gradient also deforms the symmetric structure of the streaming vortices. A threshold Reynolds number for classical streaming formation was suggested. The finite-amplitude nonlinear standing waves were also considered. Hamilton et al. [14] developed an analytical solution for the average mass transport velocity in a standing wave field between parallel plates. Hamilton et al. [15] extended their study to determine the influence of heat conduction and temperature dependence of fluid viscosity. Thermoacoustic streaming in a tube with isothermal outer wall was analyzed by Lu and Cheng [16]. Dridi et al. [17] studied the linear stability of acoustic streaming flows in laterally heated or isothermal fluids confined between two parallel horizontal infinite walls. A range of acoustic parameter values (depending on the beam width and the Grashof number) stabilizing the flow field was determined.

The present paper focuses on the irregular acoustic streaming in symmetrically heated (for horizontal walls) rectangular enclosures. A parametric study was performed in order to evaluate the effect of wall displacement amplitude, enclosure height and wall temperature on transport phenomena in the enclosure. The effects of symmetric heating on irregular streaming patterns are predicted.

ISBN: 978-988-19252-2-0
ISSN: 2078-0958 (Print); ISSN: 2078-0966 (Online)

II. PROBLEM DEFINITION

A typical air-filled two dimensional rectangular enclosure is schematically shown in Fig. 1. The left wall of the enclosure is vibrating with a frequency that induces standing waves at along the enclosure. The displacement of left wall is given by $X(t) = X_{max}\sin\omega t$. Here, X_{max} is the maximum displacement of left wall. The vibration frequency of the left wall is chosen as f = 1 kHz. The length of the enclosure is half wavelength $L=\lambda/2=173.6$ mm, and for the height of the enclosure two different value is considered, $H_1=2.8$ mm and $H_2=5.6$ mm. These values correspond to $40\delta_v$ and $80\delta_v$, respectively. Here, δ_v is the thickness of acoustic boundary layer, given by $\delta_v=(2\nu/\omega)^{1/2}$. The acoustic boundary layer thickness is approximately $\delta_v=70$ μm for the present numerical simulations. The fully compressible form of the Navier-Stokes and energy equations in 2-D Cartesian coordinate system are employed to model the transport phenomena in the enclosure considered.

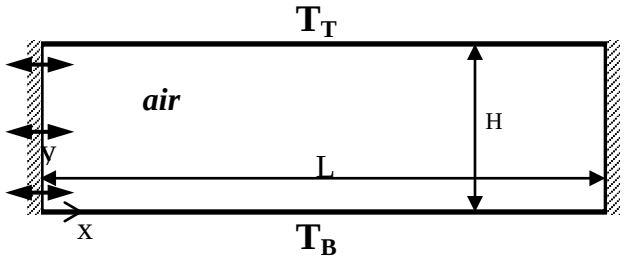

Figure 1. Problem schematic

Table 1 lists the cases studied in order to determine the influence of acoustic streaming on convective heat transfer in symmetrically heated enclosures. The dimensionless channel width H/δ_v, the maximum displacement amplitude of the left wall and the horizontal wall temperatures are presented in the table.

Table 1: Summary of the cases simulated

Case	H/δ_v	X_{max} (μm)	$T_B = T_T$ (K)
1	40	60	300
2		250	300
2a			310
2b			320
2c			350
3	80	100	300
3a			310
3b			320
3c			350

III. MATHEMATICAL MODEL

A. Transport Equations

The fully compressible form of the Navier-Stokes and energy equations in 2-D Cartesian coordinate system are employed to model the transport phenomena in the enclosure considered:

$$\frac{\partial\rho}{\partial t}+\frac{\partial(\rho u)}{\partial x}+\frac{\partial(\rho v)}{\partial y}=0 \tag{1}$$

$$\rho\frac{\partial u}{\partial t}+\rho u\frac{\partial u}{\partial x}+\rho v\frac{\partial u}{\partial y}=-\frac{\partial p}{\partial x}+\frac{\partial\tau_{xx}}{\partial x}+\frac{\partial\tau_{xy}}{\partial y} \tag{2}$$

$$\rho\frac{\partial v}{\partial t}+\rho u\frac{\partial v}{\partial x}+\rho v\frac{\partial v}{\partial y}=-\frac{\partial p}{\partial y}+\frac{\partial\tau_{yy}}{\partial y}+\frac{\partial\tau_{xy}}{\partial x} \tag{3}$$

$$\frac{\partial E}{\partial t}+\frac{\partial}{\partial x}\left[(E+p)u\right]+\frac{\partial}{\partial y}\left[(E+p)v\right]=$$
$$\frac{\partial}{\partial x}\left[u\tau_{xx}+v\tau_{xy}\right]+\frac{\partial}{\partial y}\left[u\tau_{xy}+v\tau_{yy}\right]-\frac{\partial q_x}{\partial x}-\frac{\partial q_y}{\partial y} \tag{4}$$

The effect of gravity is not considered in the present numerical simulations. Here

$$E=\frac{p}{\gamma-1}+\frac{1}{2}\rho(u^2+v^2) \tag{5}$$

The components of the stress tensor τ are:

$$\tau_{xx}=\frac{4}{3}\mu\frac{\partial u}{\partial x}-\frac{2}{3}\mu\frac{\partial v}{\partial y}\qquad \tau_{yy}=\frac{4}{3}\mu\frac{\partial v}{\partial y}-\frac{2}{3}\mu\frac{\partial u}{\partial x}$$
$$\tau_{xy}=\mu\left(\frac{\partial u}{\partial y}+\frac{\partial v}{\partial x}\right) \tag{6}$$

where μ is the shear viscosity. The components of the heat-flux vector are written as:

$$q_x=-k\frac{\partial T}{\partial x}\qquad q_y=-k\frac{\partial T}{\partial y} \tag{7}$$

where k is thermal conductivity and T is temperature. The ideal gas law is;

$$p=\rho RT \tag{8}$$

Where R (= 287 J/kgK) is the gas constant of air.

B. Numerical Model

An explicit finite volume approach is used to solve the discretized form of the governing equations. The convective terms are discretized using a Flux-Corrected Transport (FCT) algorithm while the diffusion terms are discretized by a central-difference scheme. The FCT approach [18] for solving the convective transport terms allows higher order

ISBN: 978-988-19252-2-0
ISSN: 2078-0958 (Print); ISSN: 2078-0966 (Online)

accuracy and the ability to control numerical diffusion within the finite-difference grid. Time-step splitting approach is used to include the convection, diffusion and compressibility effects.

C. Initial and Boundary Conditions

The boundary conditions of the problem under investigation are:

$u(0,y,t) = \omega X_{max} \cos\omega t$ $\quad$ $v(0,y,t) = 0$

$u(L,y,t) = v(L,y,t) = 0$

$u(x,0,t) = v(x,0,t) = 0$

$u(x,H,t) = v(x,H,t) = 0$

$$\frac{\partial T}{\partial x}(0,y,t) = \frac{\partial T}{\partial x}(L,y,t) = 0$$

$T(x,0,t) = T_B$ $\quad$ $T(x,H,t) = T_T$

The initial conditions are:

$p(x,y,0) = 101325$ Pa; $T(x,y,0) = 300$ K;
$\rho(x,y,0) = 1.1768$ kg/m^3

The boundary conditions for the higher order FCT-based solutions of the Navier-Stokes equations require a rigorous formulation. No-slip boundary conditions are used for velocity on all walls. The wall boundary conditions for density are updated using the formulation developed by Poinsot and Lele [19] based on characteristic wave relations. The use of this method avoids over-specification of variables and incorrect extrapolations from interior point values.

IV. RESULTS

Case 1 is an isothermal base case simulation and its results are compared with the existing literature for code validation. The horizontal wall temperatures are kept at 300 K in Case 1. The maximum wall displacement amplitude is 60 μm for these cases. Fig. 2 depicts the cycle - averaged flow field in the enclosure for Case 1.

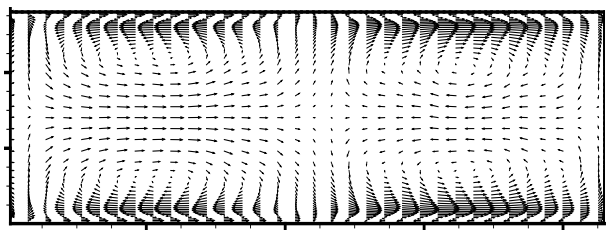

Figure 2. Streaming flow field at t = 0.04 s for Case 1.

These secondary, steady flow structures (acoustic streaming) are computed based on the average mass transport velocities defined as;

$$u_{st} = \frac{\langle \rho u \rangle}{\langle \rho \rangle} \qquad v_{st} = \frac{\langle \rho v \rangle}{\langle \rho \rangle} \tag{9}$$

Here u_{st} is x- and v_{st} is y- component of the acoustic streaming velocity. The symbol $\langle\ \rangle$ denotes time averaging. The instantaneous density, u and v values are time averaged during the 40th cycle and the streaming velocities at t = 0.04 s is obtained. By this time, the mass transport velocities reach quasi steady values and do not change with increasing number of periods. In Case 1, four circulatory flow structures (namely inner streaming) are observed at the vicinity of the horizontal walls. These structures form around the acoustic boundary layer. The vertical size of the streaming patterns observed in the middle section of the enclosure, namely outer streaming (two clockwise and two counter clockwise) is determined by the enclosure height. The length of the boundary layer and outer streaming rolls is a quarter wavelength. This flow pattern is name as classical or regular acoustic streaming.

The variation of the x- component of the streaming velocity along the enclosure semi-height at x=3L/4 for Case 1 is depicted in Fig. 3. In order to demonstrate the grid independency of the numerical estimations, the streaming velocity values from the simulations performed using a coarser (81 x 91) and a denser (121 x 111) numerical mesh are added in the figure.

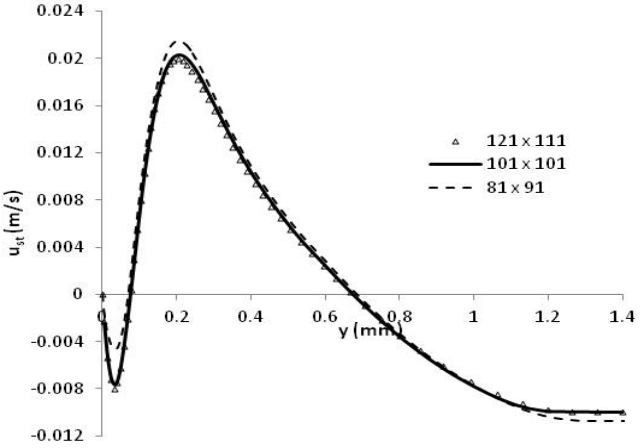

Figure 3. x- component of the streaming velocity along the enclosure semi – height (at x=3L/4) for Case 1.

Here the comparison based on the streaming (secondary flow) velocity is selected as a critical test since any error in the primary oscillatory field would be much more pronounced in the secondary flow field. The results show that 101 x 101 computational mesh structure is sufficient to resolve the flow pattern and the computations are grid independent.

Fig. 4 shows the variation of x- component of the streaming velocity along the enclosure height ($0 \le y \le H$) at x = 3L/4. The x- component of the streaming velocity (u_{st}) is non-dimensionalized by a reference streaming velocity [15] given by $u_{Ra}=3u_{max}^2/16c_0$ where u_{max} is the maximum velocity in the oscillatory flow field and c_0 is the reference speed of sound. The numerical predictions are in good agreement with Hamilton et al. [14]'s results.

ISBN: 978-988-19252-2-0
ISSN: 2078-0958 (Print); ISSN: 2078-0966 (Online)

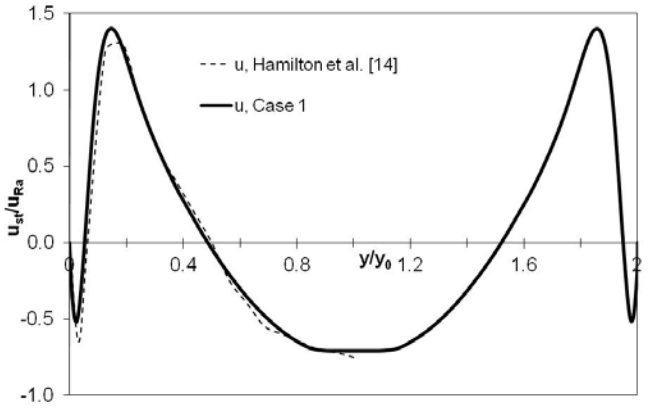

Figure 4. Variation of x- component of the streaming velocity along the enclosure height at x=3L/.

In second group of simulations (Case 2, 2a, 2b, 2c), the maximum wall displacement is increased to 250 μm. The cycle - averaged streaming fields are shown in Fig. 5 for Case 2, 2b and 2c having horizontal wall temperature values of 300 K, 320 K and 350 K, respectively. For these cases, the time required to achieve time independent quasi steady flow velocities is 0.04 s. The irregular streaming flow in the form of multiple vortical patterns is observed in the enclosure in Fig. 5(a). The acoustic streaming field is quite symmetric with respect to the horizontal and the vertical mid-planes. This type of flow pattern is associated with strongly distorted, sharp pressure wave form.

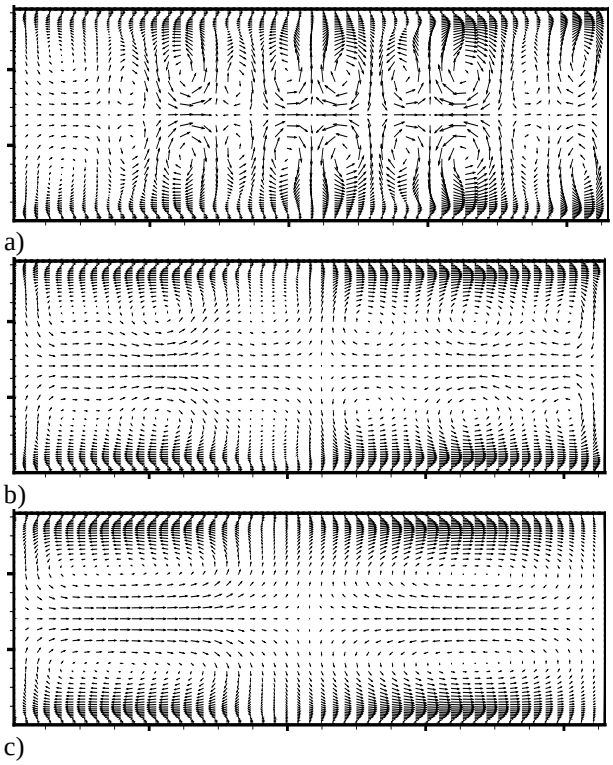

Figure 5. Cycle averaged flow field at t = 0.04 s for a) Case 2, b) Case 2b and c) Case 2c.

Fig. 6 depicts the pressure waves estimated for Cases 2, 2a, 2b and 2c. The increase of the horizontal wall temperatures in Case 2b (Fig. 5(b)), reduces the number of streaming vortices compared to the flow pattern found in Fig. 5(a) for the case of unheated walls. Three clockwise and three counter clockwise circulation core characterize the streaming field in the bottom or top half of the enclosure. A further increase of the wall temperatures (T_B=T_T = 350 K) in Case 2c reproduces the classical acoustic streaming structure in the enclosure. Both inner and outer streaming patterns are present in Case 2, 2b and 2c.

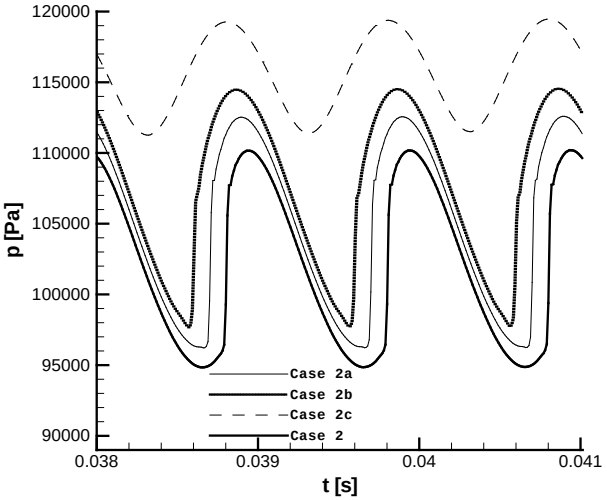

Figure 6. Temporal variation of the left wall pressure near the end of 40th cycle for Case 2, 2a, 2b and 2c.

The effect of horizontal wall temperatures on x- component of the streaming velocity profiles for Case 2, 2a, 2b and 2c having horizontal wall temperatures of 300 K, 310 K, 320 K and 350 K, respectively are presented in Fig. 7.

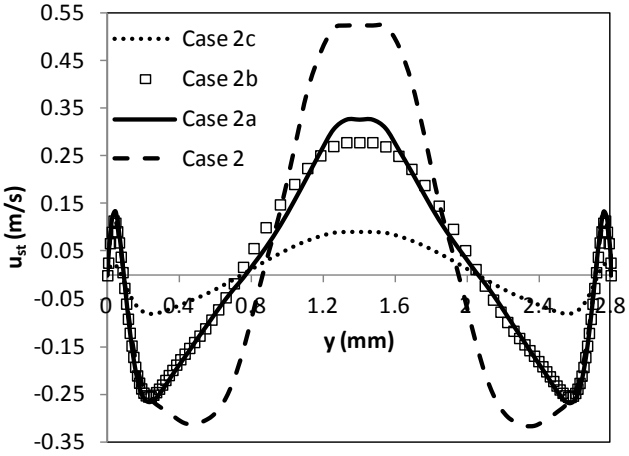

Figure 7. Variation of the x- component of the streaming velocity along the enclosure height at x=3L/4 for Case 2, 2a, 2b and 2c.

The profiles are plotted along the vertical planes at x=L/4 for Case 2a and 2b, at x=50 mm for Case 2 and at x=30 mm for Case 2c. Each plane cross the core of the strongest circulation in the left half of the enclosure. The maximum absolute velocity magnitudes are computed for Case 2 with unheated horizontal walls. In Case 2a, 2b and 2c, the

ISBN: 978-988-19252-2-0
ISSN: 2078-0958 (Print); ISSN: 2078-0966 (Online)

maximum streaming velocities are significantly reduced with increasing wall temperatures.

In order to investigate the effect of enclosure height on acoustic streaming patterns four additional cases for the 5.6 mm high enclosure are numerically simulated. The maximum wall displacement is chosen as 100 μm for Cases 3, 3a, 3b, and 3c.

Fig. 8(a), 8(b) and 8(c) show the streaming field for Case 3, 3b and 3c, respectively.

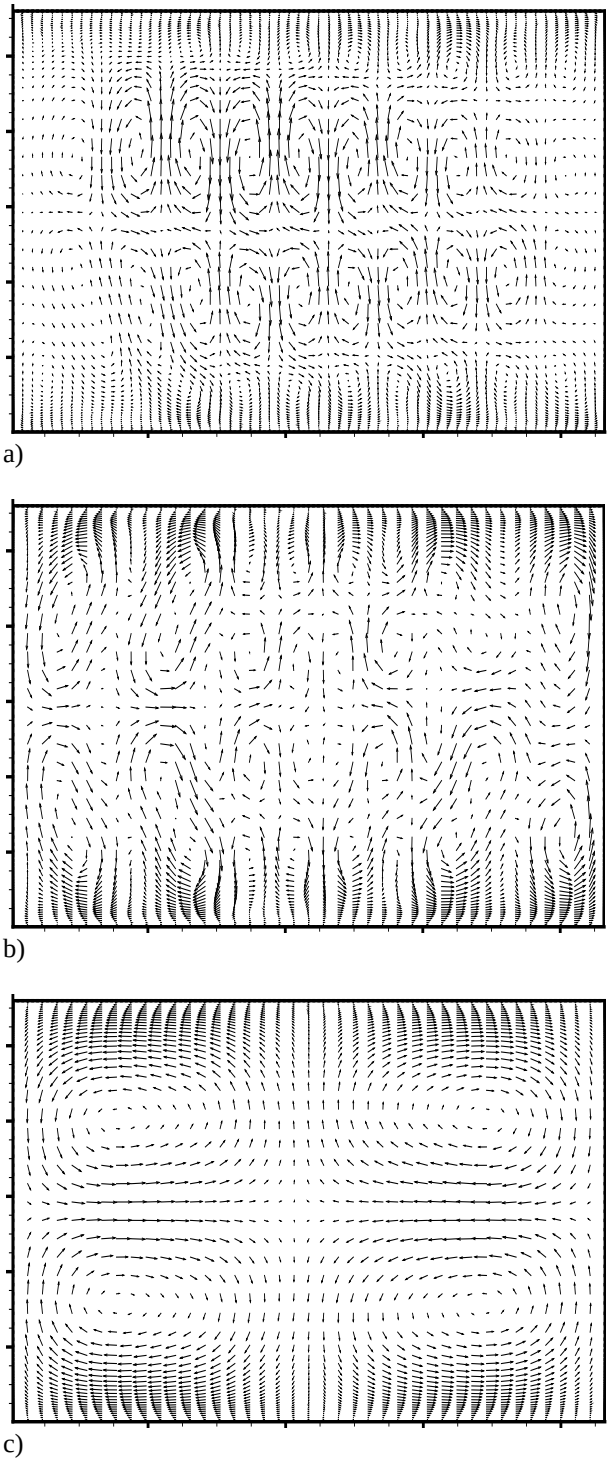

Figure 8. Cycle averaged flow field at t = 0.05 s for a) Case 3, b) Case 3b and c) Case 3c.

For these cases, the time independent behavior is achieved at 50th acoustic cycle and the time averaged flow fields are plotted at t=0.05 s. The nature of the predicted flow patterns for Case 3 and 3c are quite similar to the flow structures obtained in Case 2 and 2c. In Case 3c, the increase of the top and the bottom wall temperature to 350 K significantly reduces the number of streaming vortices as in Case 2c.

V. CONCLUSIONS

The influences of temperature gradients on irregular acoustic streaming in enclosures heated from the top and the bottom walls are computationally investigated. The heating of the enclosure horizontal walls strongly change the acoustic streaming pattern and velocity. The streaming form is determined by the pressure and the density distributions in the enclosure.

REFERENCES

[1] P. Merkli and H. Thomann, Transition to turbulence in oscillating pipe flow, J. Fluid Mech., vol. 68 (3), pp. 567–575, 1975.

[2] S. Moreau, H. Bailliet and J.C. Valiere, Measurements of inner and outer streaming vortices in a standing waveguide using laser doppler velocimetry, J. Acoust. Soc. Am., vol. 123 (2), pp. 640–647, 2008.

[3] M. Kawahashi and M. Arakawa, Nonlinear phenomena induced by finite-amplitude oscillation of air column in closed duct, JSME Int. J., vol. 39 (2), pp. 280–286, 1996.

[4] T. Yano, Turbulent acoustic streaming excited by resonant gas oscillation with periodic shock waves in a closed tube, J. Acoust. Soc. Am., vol. 106 (1), pp. L7–L12, 1999.

[5] A. Alexeev and C. Gutfinger, Resonance gas oscillations in closed tubes: Numerical study and experiments, Phys. Fluids, vol. 15 (11), pp. 3397–3408, 2003.

[6] M.K. Aktas and B. Farouk, Numerical simulation of acoustic streaming generated by finite-amplitude resonant oscillations in an enclosure, J. Acoust. Soc. Am., vol. 116 (5), pp. 2822–2831, 2004.

[7] M.W. Thompson and A.A. Atchley, Simultaneous measurement of acoustic and streaming velocities in a standing wave using laser Doppler anemometry, J. Acoust. Soc. Am., vol. 117 (4), pp. 1828–1838, 2005.

[8] M.W. Thompson, A.A. Atchley and M.J. Maccarone, Influences of a temperature gradient and fluid inertia on acoustic streaming in a standing wave, J. Acoust. Soc. Am., vol. 117 (4), pp. 1839–1849, 2005.

[9] M. Nabavi, M.H.K. Siddiqui and J. Dargahi, Simultaneous measurement of acoustic and streaming velocities using synchronized PIV technique, Meas. Sci. Technol., vol. 18, pp. 1811–1817, 2007.

[10] M. Nabavi, M.H.K. Siddiqui and J. Dargahi, Experimental investigation of the formation of acoustic streaming in a rectangular enclosure using a synchronized PIV technique, Meas. Sci. Technol., vol. 19, pp. 065405, 2008.

[11] D.R. Lee and B.G. Loh, Smart cooling technology utilizing acoustic streaming, IEEE Trans. Comp. Pack.

ISBN: 978-988-19252-2-0
ISSN: 2078-0958 (Print); ISSN: 2078-0966 (Online)

Tech., vol. 30 (4), pp. 691–699, 2007.
[12] M. Nabavi, M.H.K. Siddiqui and J. Dargahi, Influence of differentially heated horizontal walls on the streaming shape and velocity in a standing wave resonator, Int. Comm. Heat Mass Transfer, vol. 35, pp. 1061–1064, 2008.
[13] M. Nabavi, M.H.K. Siddiqui and J. Dargahi, Effects of transverse temperature gradient on acoustic and streaming velocity fields in a resonant cavity, Appl. Phys. Lett., vol. 93, pp. 051902, 2008.
[14] M.F. Hamilton, Y.A. Ilinskii and E.A. Zabolotskaya, Acoustic streaming generated by standing waves in two-dimensional channels of arbitrary width, J. Acoust. Soc. Am., vol. 113 (1), pp. 153–160, 2003.
[15] M.F. Hamilton, Y.A. Ilinskii and E.A. Zabolotskaya, Thermal effects on acoustic streaming in standing waves, J. Acoust. Soc. Am., vol. 114 (6), pp. 3092–3101, 2003.
[16] G.Q. Lu and P. Cheng, Thermoacoustic streaming in a tube with isothermal outer surface, Int. J. Heat Mass Transfer, vol. 48, pp. 1599–1607, 2005.
[17] W. Dridi, D. Henry and H. BenHadid, Influence of acoustic streaming on the stability of an isothermal or laterally heated fluid layer, C. R. Mecanique, vol. 335, pp. 175–180, 2007.
[18] E. S. Oran and J.P. Boris, Numerical Simulation of Reactive Flows, 2nd ed., pp. 275 – 284, Cambridge University Press, Cambridge, England, 2000.
[19] T.J. Poinsot and S.K. Lele, Boundary conditions for direct simulations of compressible viscous flows, J. Comput. Phys., vol. 101, pp. 104–129, 1992.

ISBN: 978-988-19252-2-0
ISSN: 2078-0958 (Print); ISSN: 2078-0966 (Online)